Dynamic simulation of pure hydrogen production via ethanol steam reforming in a catalytic membrane reactor

Ali Hedayati, Olivier Le Corre, Bruno Lacarrière, Jordi Llorca

Dynamic Simulation of Pure Hydrogen Production via ethanol Steam Reforming in a Catalytic Membrane Reactor

Ali Hedayati*[ab], Olivier Le Corre[a], Bruno Lacarrière[a], Jordi Llorca[b]

[a] Department of energy systems and environment, Ecole des Mines de Nantes, 4 Rue Alfred Kastler,44307 Nantes, France. ali.hedayati@mines-nantes.fr

[a] Department of energy systems and environment, Ecole des Mines de Nantes, 4 Rue Alfred Kastler, 44307Nantes, France. Olivier.Le-Corre@mines-nantes.fr

[a] Department of energy systems and environment, Ecole des Mines de Nantes, 4 Rue Alfred Kastler, 44307Nantes, France. Bruno.Lacarriere@mines-nantes.fr

[b] Institute of Energy Technologies, Universitat Politècnica de Catalunya, Diagonal 647, ETSEIB, 08028 Barcelona, Spain. jordi.llorca@upc.edu

***corresponding author : Ali Hedayati**:
ali.hedayati@mines-nantes.fr**,** Department of energy systems and environment, Ecole des Mines de Nantes, 4 Rue Alfred Kastler, 44307Nantes, France.
ali.hedayati@upc.edu, Institute of Energy Technologies, Universitat Politècnica de Catalunya, Diagonal 647, ETSEIB, Pav. C, 08028 Barcelona, Spain.

Abstract

Ethanol steam reforming (ESR) was performed over Pd-Rh/CeO_2 catalyst in a catalytic membrane reactor (CMR) as a reformer unit for production of fuel cell grade pure hydrogen. Experiments were performed at 923 K, 6-10 bar, and fuel flow rates of 50 to 200 µl/min using a mixture of ethanol and distilled water with steam to carbon ratio of 3. A static model for the catalytic zone was derived from the Arrhenius law to calculate the total molar production rates of ESR products, i.e. CO, CO_2, CH_4, H_2, and H_2O in the catalytic zone of the CMR (coefficient of determination R^2 = 0.993). The pure hydrogen production rate at steady state conditions was modeled by means of a static model based on the Sieverts' law. Finally, a dynamic model was developed under ideal gas law assumptions to simulate the dynamics of pure hydrogen production rate in the case of the fuel flow rate or the operational pressure set point adjustment (transient state) at isothermal conditions. The simulation of fuel flow rate change dynamics was more essential compared to the pressure change one, as the system responds much faster to such an adjustment. The results of the dynamic simulation fitted very well to the experimental

values, which proved the robustness of the simulation based on the Sieverts' law. The simulation presented in this work is similar to the hydrogen flow rate adjustments needed to set the electrical load of a fuel cell, when fed online by the pure hydrogen generating reformer studied.

Keywords:
Ethanol Steam Reforming, Pure hydrogen production, Membrane reactor, Dynamic simulation, Sieverts' law

Highlights:

- Ethanol steam reforming (ESR) experiments were performed in a Pd-Ag membrane reactor
- The model of the catalytic zone of the reactor was derived from the Arrhenius law
- The permeation zone (membrane) was modeled based on the Sieverts' law
- A dynamic model was developed under ideal gas law assumptions
- Pressure and fuel flow rate adjustments were considered for dynamic simulation

1. Introduction

Renewable energy resources are now considered as one of the fastest and most feasible solution to achieve the targets of clean electricity production; however, some challenges such as dependency on the geographical and local conditions and infrastructures, and transmission of produced electricity to the end users remain among the challenges to be encountered. In this regard, on-site electricity production at the place/time where needed is beneficial.

Being compatible with modern energy carriers such as hydrogen, fuel cells are considered as the efficient (45-50% electrical efficiency) and environmentally friendly energy convertors of the future power generation systems [1–3]. Fuel cells have proved potentials in different applications and can be applied in sub-MW size at any condition, independent from geographical factors such as local climate conditions. Although production of hydrogen-rich gases can offer flexible fuels for fuel cells [4], the pollution-free efficient performance of a fuel cell is reached when pure hydrogen is used [5]. Accordingly, the main challenge remains in the requirements of the special installations and infrastructures for production, distribution, and delivery of hydrogen as it is needed in highly pure state [6]. Production of hydrogen – for example via reforming processes – at the same place/time needed can make pure hydrogen storage/transportation unnecessary [7].

The use of renewable biofuels such as bio-ethanol as a source of hydrogen is highly beneficial due to the higher H/C ratio, lower toxicity, and higher safety of storage that distinguishes ethanol over other substrates. Bio-ethanol is cheaply and easily obtained from biomass and organic waste and can be used directly in catalytic steam reforming processes to produce hydrogen since it contains large amounts of water [8]. Concerning the production of fuel cell grade hydrogen, the application of catalytic membrane reactors (CMRs) is beneficial where the production and separation of hydrogen from the mixture of produced gases take place in the same reactor vessel simultaneously. In the case of Pd-Ag metallic membrane reactors, hydrogen purity up to 99.999% is obtained, which is suitable for direct low-temperature fuel cell feeding [9,10].

The application of the CMRs in pure hydrogen production (as a reformer unit) is still under investigation. The effect of the co-presence of steam reforming bybroducts (CO, H_2O, CO_2 and CH_4) on the performance of the membrane in terms of pure hydrogen permeation rate is still a

challenge to be overcome. Hou et al. [11] reported that the hydrogen inhibition effect of CO, CO_2, and H_2O in the case of a Pd-Ag membrane could be classified as $H_2O>CO>>CO_2$ in terms of the competitive adsorption capability of the gases on the Pd-Ag membrane surface. In the study by Unemoto et al. [12] the comparison between CO, CO_2, and H_2O showed that at T<600 K, CO had the strongest influence on the hydrogen permeability of the Pd membrane. They suggested that at T>873 K, the effect of co-existence of other species for a membrane with a thickness higher than 10 μm is negligible. On the contrary, Patrascu and Sheintuch [13] concluded that the effect of very small amount of CO on hydrogen permeation inhibition could be notable even in presence of H_2O. The strong effect of low concentration of CO on the membrane permeation behavior at different temperatures was reported also in other studies [14–18]. Catalano et al. [19] stated that CH_4 acted as inert gases in terms of hydrogen inhibition. Barreiro et al. [20] showed that the hydrogen flux was reduced in presence of water at 593-723 K, while CO_2 had no influence on the permeation rate of hydrogen.

Overall, the literature does not provide a consistent idea on the hydrogen inhibition phenomenon due to the competitive adsorption of CO and H_2O on the surface of the metallic Pd membrane, the effect of reverse reactions of water gas shift (WGS) and methane steam reforming (MSR), and the effect of operating at high pressure and temperature in the real atmosphere of the ESR. It is not totally agreed if CO_2 and CH_4 are considered as inert gases as their reactions with water via reverse WGS and MSR can lead to a more complicated situation regarding the influence on the hydrogen permeation. According to the review given by Cornaglia et al. [21], it can be understood that the hydrogen inhibition phenomenon caused by the ESR products especially in presence of H_2O, is a very complicated issue. It is inevitable to study each fuel reformer system specifically in terms of the properties of the membrane, operating conditions, and the composition of the fuel fed into the reformer reactor.

If a fuel cell is fed online by pure hydrogen generating system (hereafter referred to as "reformer"), the dynamics of pure hydrogen supply must be fitted to the load variations (dynamic behavior) of a fuel cell. Considering the dynamic energy demand of an end user – for example a building – a reformer must be able to realize and track the dynamic electrical output of the fuel cell in charge of electricity supply of the end user. Adjustment of the flow rate of pure hydrogen provided by a reformer is a crucial phase to respond promptly and aptly to the electrical load modifications of a fuel cell, aiming to optimize the whole system (reformer + fuel cell) performance. Although a few studies are reported in the literature regarding the dynamic performance of the fuel cells, the works devoted to the investigations of the dynamic performance of the online fuel reformers – corresponding to the load variation of the fuel cells – are not sufficiently reported in the literature [22].

Garcia et al. [23] developed a dynamic model for a three module reformer made up of ethanol dehydrogenation, acetaldehyde steam reforming, and water gas shift units for feeding hydrogen to a fuel cell. They simulated the dynamic response of the reforming unit in terms of the selectivity of the products of the ESR reaction rate to the changes in concentration of the feed (ethanol + water). The same authors in another study [24] focused on the controllability and the dynamics simulation of the same system as they reported in [23] by acting on the feed concentration at isothermal conditions. A dynamic numerical model for the methane fuel processor of a PEMFC was developed by Funke et al. [25] aiming at optimizing the reaction conditions and heat integration especially during start up, shut down, and load change. The effect of two constructions (the reactor and the evaporator with and without thermal coupling) on the temperature profile, reaction rates, and methane conversion was investigated and it was reported that hydrogen yield is higher when the reactor and the evaporator are not thermally coupled. John and Schroer [26] presented a dynamic model of a methane steam reformer for a residential fuel cell system. The dynamic model covered the full operating range including the

startup and shut down, and described the dynamics of the hydrogen yield and thermal behavior of the reformer when the flow rate of water or natural gas changed. The thermal system was affected by increasing the flow rate of the water. Higher hydrogen yield and lower methane concentration at the outlet were reported at higher temperature, i.e. lower concentration of inlet water. A dynamic model for an interconnected reformer and PEMFC stack was developed by Stamps and Gatzke [27] with emphasis on the influence of various design and operating parameters on system performance. It was concluded that operating at higher temperature results in higher system performance.

A dynamic modeling study of a catalytic steam reformer by Kvamsdal et al. [28] showed that the steam or gas (CO, CO_2, H_2, and CH_4) supply interruption affects the reactor wall temperature, which can directly lead to material failure or coke formation. Lin et al. [29] modeled the dynamics of an experimental multi stage methane reformer in charge of providing hydrogen to a PEMFC to design a control system to provide the responsiveness of the fuel reformer to the alterations in the hydrogen demand. The response of the fuel reformer to changes in the process variables such as CH_4 feed flow rate, H_2O/CH_4 feed ratio, O_2/CH_4 feed ratio and the reformer inlet temperature was studied. Tsourapas et al. [30] presented a dynamic model based on thermodynamics and energy balance for a JP5 fuel reformer in connection with a membrane separator (SEP) and a PEM fuel cell to investigate the effects of the operating set point of SEP on the overall system efficiency. They concluded that the open loop response of the system is shown to be satisfactory in terms of the response time and hydrogen production. It was shown that there is a trade-off between the SEP efficiency and the overall efficiency of the system.

In another work by Koch et al. [10], a dynamic model of an ethanol steam reformer (as the fuel reformer for pure hydrogen production to feed a PEMFC) was developed to implement an adaptive and predictive control. The static behavior of the reformer system was described by

means of several maps developed in Matlab. Further, the dynamics of the fuel reformer in connection with a PEMFC by acting upon reactor pressure and feed flow rate (ethanol + water) was studied. They proposed an efficient controller that reduced the response time of the reformer by a factor of 7 down to 8 s in terms of following the dynamics of a fuel cell load by acting simultaneously on the fuel flow rate and pressure. However, such advanced controllers require internal models and simulations for further development.

The purpose of this paper is to present a simpler approach mainly based on physical laws (adapted Arrhenius model, mass balance, ideal gas law, and Sieverts' law). Such a model can be applied for the development of controllers, which is out of the scope of the paper. A dynamic model of a reforming system (the CMR) is given to simulate the dynamics of the pure hydrogen production rate at unsteady state conditions (between two steady state points) under fuel flow rate and pressure set-up steps. The model considers the kinetics of the catalytic reforming reactions regarding the molar production of ESR products, especially hydrogen inside the reactor at unsteady operating conditions. Moreover, the dynamic simulation is based on the real dynamic experiments using a Pd-Ag membrane reactor module (where production and separation of hydrogen takes place in the same reactor) for production of fuel cell grade hydrogen via ethanol steam reforming. Additionally, application of the CMR makes it possible to investigate the effect of the byproducts of the ESR (CO, CO_2, H_2O, and CH_4) on the performance of a real case Pd-Ag membrane based on the observed reaction kinetics (concentration of the ESR products). The latter is an important factor in monitoring and simulation of the performance of the membrane in ESR environment so that many works have been reported on the investigation of the effect of the gaseous byproducts on the permeation behavior of the membranes.

2. Materials and methods

2.1. Experimental

The Pd-Rh/CeO_2 catalyst (0.5% Pd – 0.5% Rh) was deposited over cordierite pellets of about 1 mm following the procedure described by López et al. [31]. When ESR is performed over Pd-Rh/CeO_2 catalyst, the major reforming reactions are [32,33]:

$$C_2H_5OH \rightarrow H_2 + CO + CH_4 \quad (1)$$

$$CO + H_2O \leftrightarrows H_2 + CO_2 \quad (2)$$

$$CH_4 + 2H_2O \leftrightarrows 4H_2 + CO_2 \quad (3)$$

$$C_2H_5OH + 3H_2O \leftrightarrow 2CO_2 + 6H_2 \quad (4)$$

Equations 1-3 represent the ethanol decomposition, water gas shift, and methane steam reforming reactions, respectively. Equation 4 is the overall ESR reaction.

The laboratory setup used for the ESR experiments (fuel reformer) consisted essentially of a fuel tank, a liquid pump, a CMR, a pressure transducer and a condenser. A detailed description of the reformer setup can be found in [34]. A schematic plan of the fuel reformer system is shown in Fig. 1.

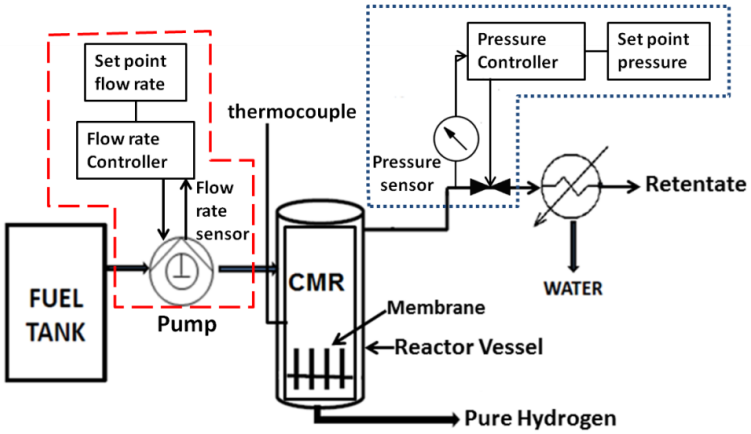

Fig. 1. Scheme of the Reformer.

The dashed and dotted lines represent the fuel flow rate and pressure controlling systems, respectively. The CMR (provided by Reb Research and Consulting [35]) was 10 in. tall and 1 in. in diameter. There were four Pd-Ag membrane tubes selective to hydrogen inside the reactor; each one 3 in. tall and 1/8 in. diameter in order to separate hydrogen from the gases produced. To perform the experiments, the reactor was filled with the catalysts so that the metallic membranes were fully covered. The retentate pressure was adjusted by a back-pressure regulator (transducer). No pressure regulation was implemented on the permeate side and no sweep gas was used so that pure hydrogen was obtained at atmospheric pressure. The flow rate of pure hydrogen (permeate) was measured with a mass flow meter and fluctuated within ±2 ml/min. The composition of retentate gases (waste gases) was analyzed on a dry basis using an online Gas Chromatograph (±3%) (Agilent 3000A MicroGC using MS 5 Å, PlotU and Stabilwax columns) every 4 minutes.

The operating conditions of the experiments under steady conditions are summarized in Table 1. The experiments were performed at isothermal conditions.

Table 1. Experimental conditions

Temperature $T^{set\ point}$ (K)	923
Pressure $P^{set\ point}$ (bar)	6-10
Fuel flow rate $F_F^{set\ point}$ (μl/min)	50-200
Steam to carbon ratio *SC*	3

At 923 K, the ESR over the Pd-Rh/CeO_2 catalyst is optimized in terms of hydrogen selectivity, hydrogen recovery, and ethanol conversion [31,32,36,37]. At SC ratio of 3, the highest value of hydrogen recovery was obtained during the experimental work that is attributed to the

availability of water for the reforming reactions. On the other hand, coke formation is less prone to occur at a higher SC ratio with respect to the stoichiometric value.

Two types of dynamic tests were performed in this study: pressure change and flow rate change. In the case of pressure change dynamic tests, both increasing and decreasing steps were considered. As presented in Fig. 2, the pressures range of 7-10 bar was selected because at these pressures the efficiency of the fuel reformer is maximum [38].

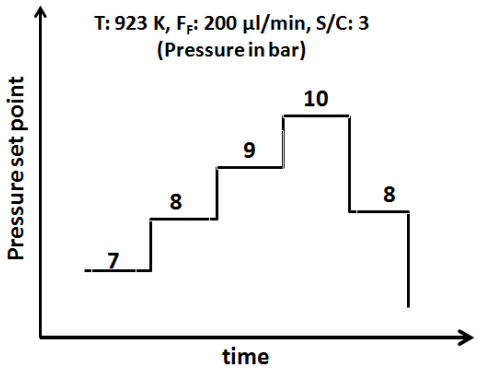

Fig. 2. Scheme of the pressure change for the dynamic tests.

Dynamic tests regarding the response of the system to the fuel flow rate changes were performed through intervals of 50 µl/min as shown in Fig. 3.

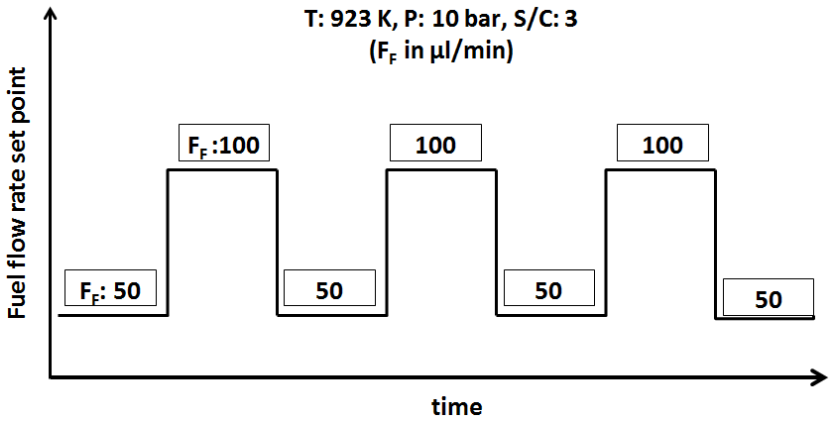

Fig. 3. Scheme of the fuel flow rate change for the dynamic tests.

The changing cycles were run more than one time to observe the durability of the performance of the reforming system. According to the membrane limitations, higher flow rates were not taken into account.

2.2. CMR isothermal model

For the modeling task, the CMR was divided into two sections, i.e. the catalytic zone, and the permeation zone (the membrane) as shown in the Fig. 4. The ESR reactions were supposed to occur in the catalytic zone, resulting in total production of the retentate gas plus the permeated hydrogen. The permeation zone (the membrane) stands for the pure hydrogen generating step for which the dynamic model was developed. The outputs of the catalytic zone model were used as the input of the static models of the permeation zone (i.e. the membrane).

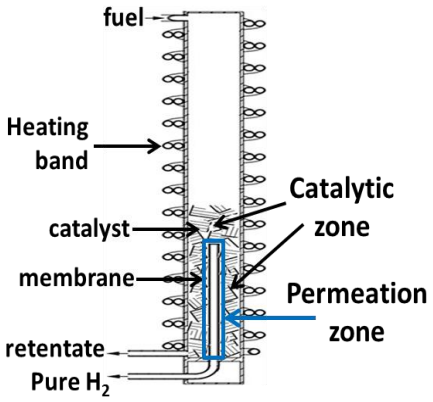

Fig. 4. The catalytic zone and the permeation zone of the CMR

It is assumed that the fuel (ethanol+water) is in its gas phase at the entrance of the volume of the CMR and the ideal gas law is applied. The CMR model is splitted into a static model and a first oder transfer function, i.e. ESR products are driven by the operating conditions (pressure and temperature) under steady state conditions.

2.2.1. Static model of the catalytic zone

A static model for the catalytic zone was developed to calculate the total molar production rate of species present in the catalytic zone of the CMR, i.e. CO, CO_2, CH_4, H_2, and H_2O as the products of the catalytic conversion of ethanol (around the membrane). The static model was derived following the Arrhenius law as a function of fuel flow rate and operating pressure in the form of:

$$\dot{n}_{specie} = f_{specie} \times exp(-\frac{g_{specie}}{RT}) \quad (5)$$

$$f_{specie} = \alpha_{specie} \times F_F^{\beta_{specie}} \quad (6)$$

$$g_{specie} = \theta_{specie} \times P + \gamma_{specie} \quad (7)$$

$\dot{n}_{specie}$ [mol/s] is the molar production rate of each species produced in the CMR via ESR over the catalyst (and around the membrane). F_F [m^3/s] and P [Pa] represent the fuel (ethanol + water) flow rate and the reactor pressure, respectively. 'f_{specie}' represents a function of fuel flow rate as pre-exponential factor, and 'g_{specie}' represents the energy of activation as a function of pressure. α_{specie}, β_{specie}, θ_{specie}, and γ_{specie} are the fitting parameters of the equations. The introduced model was applied to calculate the molar production rate of the ESR products, mainly to calculate the partial pressure of hydrogen ($P_{H2,r}$ in eq. 9) around the membrane surface (right before the permeation zone).

2.2.2. Static models of the permeation zone

The model of hydrogen permeation through the membrane at steady state was derived from the Sieverts' law. Hydrogen permeation phenomenon through a Pd-Ag membrane is explained by Sieverts' law based on the mass transfer and surface reactions principals [19,39]. As stated by the Sieverts' law, the hydrogen permeation rate through Pd-Ag membrane is a temperature activated phenomena driven by the difference between the partial pressure of hydrogen at two sides, i.e. the retentate side (inside the reactor, around the membrane) and the permeate side (right after the membrane) [31,33]:

$$J_{H2} = \frac{Q_0}{\delta} e^{\frac{-E_a}{RT}} (\sqrt{P_{H2,r}} - \sqrt{P_{H2,perm}}) \quad (8)$$

Where J_{H2} is the pure hydrogen production rate obtained via the Sieverts' law. δ is the thickness of the membrane and Q_0 is the pre-exponential factor. E_a, *R*, and T are the activation energy, universal gas constant, and temperature, respectively. $P_{H2,r}$ and $P_{H2,perm}$ are the partial pressure of hydrogen at the retentate and permeate side, respectively.

The partial pressure of hydrogen inside the reactor was calculated based on the hydrogen fraction in the gas phase assuming that the only present species in the catalytic bed (and around the membrane) are CO, CO_2, CH_4, H_2 and H_2O. Therefore:

$$P_{H2,r} = P \times y_{H2,r} \quad (9)$$

Where P and $y_{H2,r}$ represent the reactor pressure and the molar fraction of hydrogen in the catalyst bed, respectively. The reactor pressure simulation method is explained in section 2.2.3. The activation energy (E_a) and the pre-exponential factor (Q_0) are calculated by means of permeation experiments during which pure hydrogen at known temperature and pressure is purged and the permeation rate of hydrogen through the membrane is measured (atmospheric pressure at the permeate side) [40–45].

As discussed before, the published open literature offers no robust model/analysis on the effect of different species on the performance of the membrane in the real atmosphere of methane steam reforming and water gas shift reactions. It was concluded that to understand the influence of co-existence of ESR products on the permeation performance of the membrane, specific models must be developed regarding specific operational conditions of the ESR environment.

Accordingly, a model was developed for hydrogen permeation through the Pd-Ag membrane; specifically for the ESR environment at the operating conditions presented in this work. It is assumed that the concentrations of CO and H_2O affect the permeation performance of the membrane differently at different operating conditions. The hidden effect of CH_4 and CO_2 are taken into account considering the ESR reactions (eq. 1-3). Firstly, the model presented in the section 2.2.1 (catalytic zone) was used to fit the molar flow rate of the species present in the retentate gas, i.e. CO, CO_2, CH_4, H_2, and H_2O (to calculate the partial pressure of hydrogen at the retentate side).

Regarding equation 9, the activation energy (E_a) was taken from the work by Papadias et al. [46] as they used the same membrane module as the one used in this work, with the same characteristics and synthetized by the same manufacturer (REB Research & Consulting [35]).

Therefore, the term $\frac{e^{\frac{-E_a}{RT}}}{\delta}$ in eq. 9 was calculated, which is equal to 54.9 [m^{-1}]. Then, the term 'Q_0' was obtained firstly from the experimental results ($Q_0^{measure}$), and then modeled (Q_0^{model}) by means of a static model as a function of the reactor pressure (P) and fuel flow rate (F_F):

$$Q_0^{measure} = \frac{J_{H2} \times \delta}{e^{\frac{-E_a}{RT}} \times (\sqrt{P_{H2,r}} - \sqrt{P_{H2,perm}})} \quad (10)$$

$$Q_0^{model} = k_1 \times F_F \times exp(k_2 \times P) \quad (11)$$

Where 'k_i' is the fitting parameter. $P_{H2,r}$ in eq. 10 is obtained via eq. 9 by using the modeled values of the molar production rate of ESR products (eq. 5-7) to calculate the hydrogen fraction in the catalytic zone. In fact, this factor was used to fit the results of the Sieverts' law based model to the experimental ones.

Accordingly, the hydrogen permeation rate at steady state conditions was modeled to be used in the simulation of the dynamics of hydrogen permeation rate at transient conditions, i.e. between two steady state points.

2.2.3. Isothermal dynamic simulation of the permeation zone

Prior to the dynamic simulation of the permeation zone, the reactor pressure was modeled in the case of pressure set point adjustment during which the pressure valve of the reforming

systems acts on the retentate gas flow rate to adjust to a higher or lower pressure. The ideal gas law in the form of $\mathrm{PV} = \frac{\mathrm{mRT}}{\mathrm{M_W}}$ was used to model the pressure of the reactor. P, V, T, and M_W are reactor pressure, the volume of the reactor, reactor temperature, and the molar mass of the fuel mixture, respectively. 'm' is the accumulated mass of the fuel added to the reactor volume. It was assumed that the accumulation rate of the pumped fuel into the constant volume of the reactor at constant temperature, results in pressure rise as the pressure valve acts on the outlet of the system to block the retentate stream when pressure increase is required. Conversely, to decrease the pressure, the pressure valve lets the retentate gas be released, so that the inlet mass flow rate of the fuel gets lower than the outlet mass flow rate. Regardless of the action of the pressure valve on the retentate gas stream, hydrogen constantly permeates through the membrane. Therefore, the added mass to the reactor volume is the difference between the fuel flow rate, and the retentate gas flow rate plus hydrogen permeation rate, so that:

$$\frac{dm}{dt} = \dot{m}_{fuel} - \dot{m}_r - \dot{m}_{H2.perm} \quad (12)$$

Where $\dot{m}_{fuel}$ and $\dot{m}_{H2.perm}$ represent the fuel flow rate and hydrogen permeation rate, respectively, both in [kg/s]. Then, the ideal gas law is written as:

$$\frac{dP}{dt} = \left(\frac{RT}{VM_W}\right) \times \frac{dm}{dt} \quad (13)$$

Where $\frac{\mathrm{dm}}{\mathrm{dt}}$ is the rate of the accumulation of the mass in the reactor volume. In this work, the CMR is a packed bed reactor running at isothermal conditions, with negligible axial mixing. The temperature and concentration difference is neglected, so that the models are considered as ideal plug flow pseudo-homogenous ones [47].

The dynamic simulation was performed to predict the dynamic behavior of the pure hydrogen production rate (permeate zone) in the transient periods during which the reforming system alters between two steady state points, as a result of the fuel flow rate or operating pressure set point adjustments. To develop the dynamic model of the permeate zone, a first order function was used:

$$\frac{J_{H2}^{D}}{F_F} = \frac{J_{H2}}{1+\tau s} \quad (14)$$

J_{H2}^{D} is the pure hydrogen production rate obtained by the dynamic model. The superscript "*D*" stands for the dynamic model. J_{H2} represents the hydrogen permeation rate calculated via the static model based on the Sieverts law, considering every single operating point as steady state. The time constant is presented as τ. The measured dynamic of fuel flow rate was faster than the sampling time (1 second). Therefore, the fuel flow rate is always equal to its set point value:

$$F_F = F_F^{set\ point} \quad (15)$$

Finally, equation 14 is written as:

$$\frac{J_{H2}^{D}}{F_F^{set\ point}} = \frac{J_{H2}}{1+\tau s} \quad (16)$$

Where $\mathrm{F_F^{set\ point}}$ is the fuel flow rate set point (see Fig. 3).

The simulation was performed by means of Ordinary Differential Equation (O.D.E) solver.

3. Results and discussion

Least Square Method (LSM) was applied to obtain all the fitting parameters regarding the static models. The time constant was estimated from a set of trials and errors.

3.1. Static models of the permeation zone

The products of ESR (H_2, CO, CO_2, CH_4, and H_2O) and the pure hydrogen permeation rate was modeled at four different fuel flow rates, i.e. 50, 100, 150, 200 µl/min and three different pressures (6, 8, and 10 bar). As mentioned before, the molar production rate of all the ESR products was needed in order to calculate the partial pressure of hydrogen in the catalytic zone (around the membrane). The calculated molar production rates of the ESR products (catalytic zone) are presented in Fig. 5. The dashed lines represent the 10% error (discrepancy between experiment and measurement). The x-axis (modeled) and y-axis (measured) are referred to the values calculated by the static model and obtained via experiments, respectively.

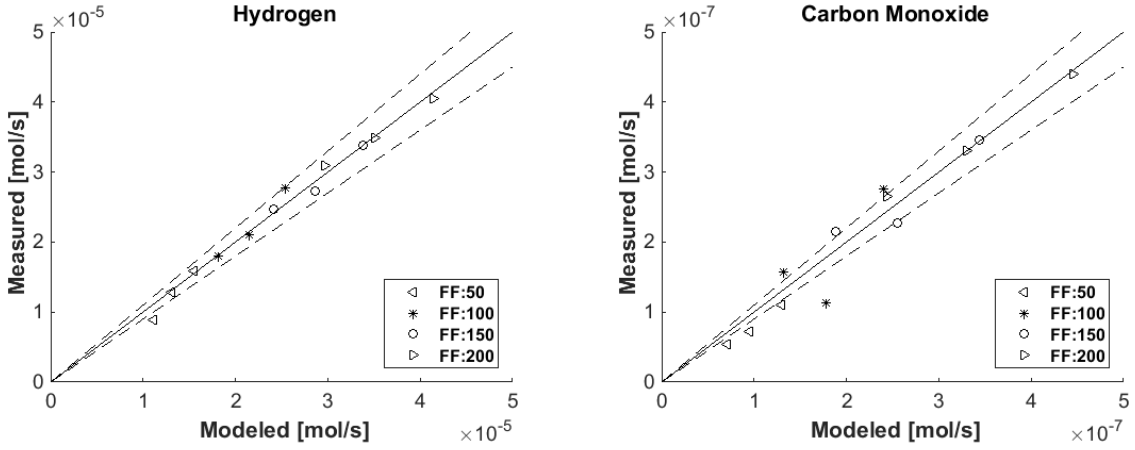

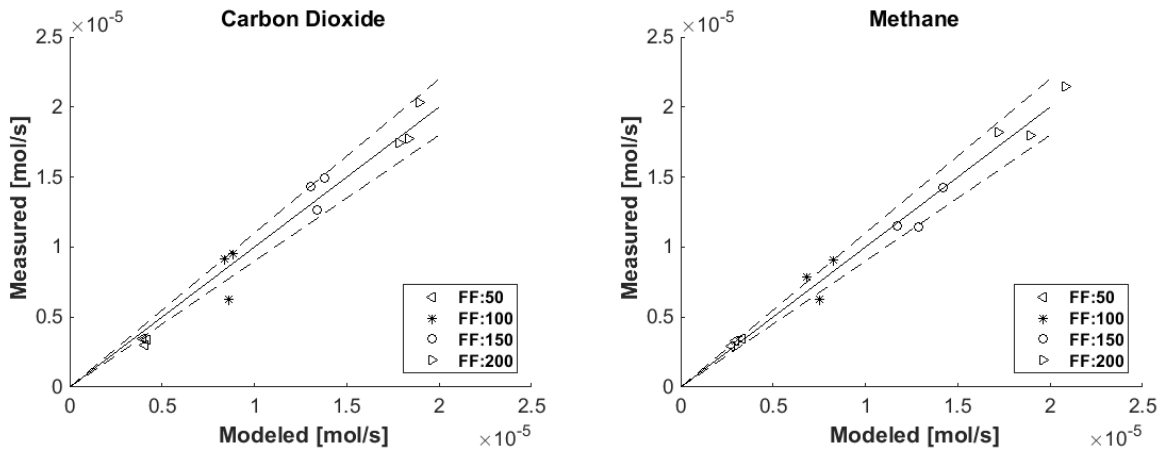

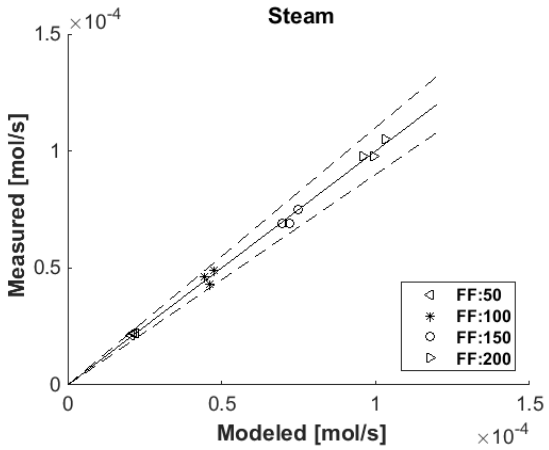

Fig. 5. Parity plots of the ESR products calculated by the static model (eq. 5-7).

The modeled values could fit the experimental results within the 10% error, especially in the case of production rate of hydrogen. The values of the fitting parameters (eq. 6 and 7) for all the gases are given in Table 2.

Table 2. Fitting parameters of the static model for the ESR products production rate model (eq. 6 and 7)

specie	α_{specie} [$mol.m^{-3}$]	β_{specie} [-]	θ_{specie} [$J.mol^{-1}.Pa^{-1}$]	γ_{specie} [$J.mol^{-1}$]	R^2
H_2	1.0873	0.7096	8.3800×10^{-7}	-0.0665	0.9954
CO	75.5364	0.8930	-1.5028×10^{-6}	-4.2727	0.9849
CO_2	133.8928	1.0915	-1.4717×10^{-7}	1.1520	0.9911
CH_4	560.2602	1.3303	-4.7941×10^{-7}	3.7000	0.9950
H_2O	226.0976	1.1131	-1.7989×10^{-7}	2.6771	0.9992

Keeping in mind equations 5-7, it can be seen that the values of $P\times\theta$ are very small compared to γ, except in the case of hydrogen. As mentioned before, the most effective factor on the hydrogen permeation is the partial pressure of hydrogen in the reactor; hence, the value of $P\times\theta$ is higher in this case. The same explanation can be given regarding the parameter β. In the case of hydrogen, the effect of pressure in the CMR configuration is dominant in comparison with the fuel flow rate, resulting in the smallest value of β in the case of hydrogen. Conversely, the value of β in the case of CH_4 is the highest among the gases because the only source of CH_4 is the ethanol decomposition reaction (eq. 1). At complete ethanol conversion, the higher the fuel flow rate is, the higher the production rate of CH_4 is. The value of β in the case of H_2O is nearly one, which is very relevant since the ESR reaction were performed at SC=3, where there is a large amount of excess water. It can be concluded that the molar flow rate of water is proportional to the inlet molar flow rate of water in the fuel mixture (ethanol + water). At SC=3, a large portion of the inlet water (70-90%) leaves the reactor in the form of steam as unreacted water. The value of θ in the case of CO is one order of magnitude smaller than other gases, which is attributed to the very small amount of CO detected at the outlet of the reactor. The values of θ proves that at higher pressures, less byproducts (CO, CO_2, CH_4, and H_2O) and more

hydrogen are generated, which is totally in agreement with the experimental results and the aim of application of the CMR, where ESR reactions are promoted (the shift effect).

The value of the pre-exponential factor model (eq. 11) showed a good correlation (R^2=0.91) with the calculated values (Fig. 6) except at P=6 bar; this is interpreted to the fact that at this pressure the membrane starts to be effective for hydrogen separation.

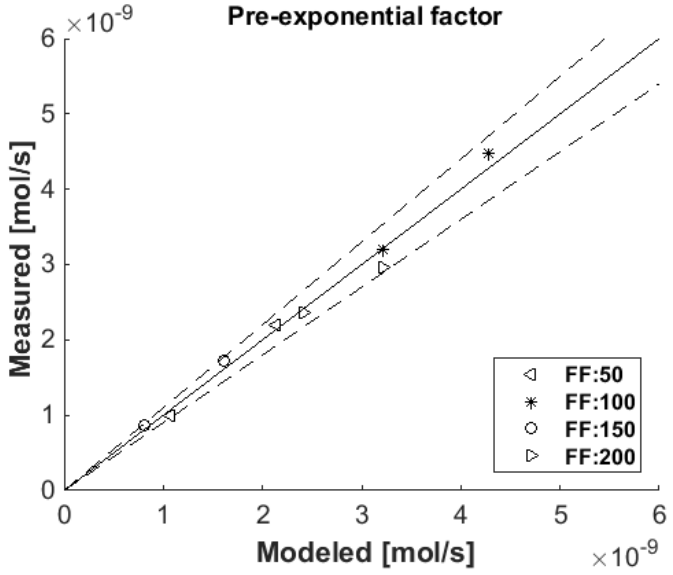

Fig. 6. The result of the pre-exponential factor model (eq. 11) at P>6 bar. The dashed lines show the 15% error range.

The values at P=6 bar are not presented due to membrane diffusion limitation at pressures lower than 6 bar. The fitting parameters considering the static models for the permeation zone (eq. 11) are given in Table 3.

Table 3. Fitting parameters of the pre-exponential factor model (eq. 11)

Parameter	k_1	k_2	R^2
value	0.602	-3.4823×10^{-6}	0.91
Unit	$[mol.m^{-2}.Pa^{-0.5}]$	$[Pa^{-1}]$	[-]

Regarding the value of k_2, the diverse effect of pressure is obvious (see eq. 11). This is attributed to the fact that at higher pressure, the concentration of hydrogen is higher around the membrane (permeation zone) leading to the lower concentration of the other gases, which directly means that the permeation performance of the membrane is less affected. This is completely in agreement with the experimental results and the assumption of the negative effect of the byproducts of the ESR reactions on the permeation behavior of the Pd-Ag membrane.

The result of the Sieverts' law model (permeation zone) is shown in Fig. 7 (P>6 bar; R^2=0.86). The partial pressure of hydrogen in the reactor (obtained based on the molar production rates of the ESR products calculated by the Arrhenius based static model) was used in the Sieverts' law to obtain the pure hydrogen permeation rate.

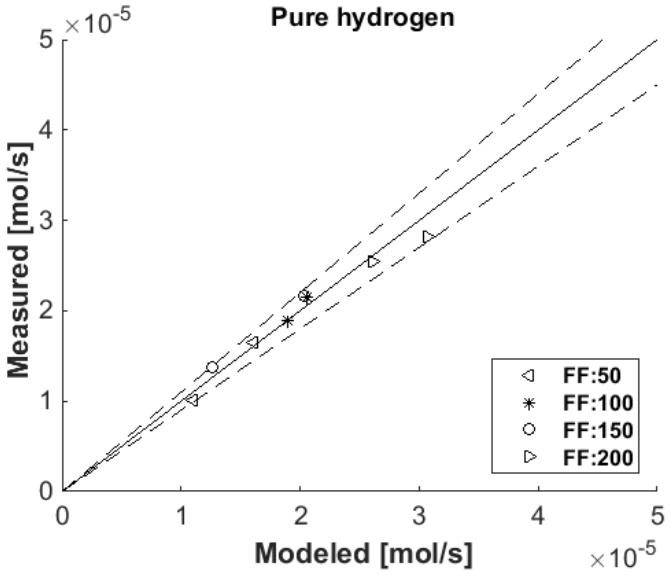

Fig. 7. Parity plots of the hydrogen permeation rate obtained by the Sieverts' law model

3.2. Isothermal Dynamic simulation

3.2.1. Pressure change simulation

To develop the dynamic model of the reforming system in the case of pressure change, firstly, the reactor pressure was simulated. Keeping in mind the configuration of the CMR, when the pressure of the reactor is set at a higher value, the outlet of the reactor is blocked so that the inlet fuel is added to the volume of the reactor to increase the pressure gradually with time. When the pressure is increased, the flow rate of the retentate gas ($\dot{m}_r$) is zero (see eq. 12). On the contrary, when reactor pressure is set at a lower value, the pressure valve is opened so that gas is released leading to sudden pressure drop in the reactor. The different behavior of the system during pressure increasing and decreasing steps is due to the different act of the pressure controlling system on the pressure valve (see Fig. 1). Therefore, the dynamics of the

system pressure control differ in different steps. The importance of such a performance lies in the dependency of pure hydrogen permeation rate through the membrane on the partial pressure of hydrogen in the reactor. The simulated pressure change behavior of the reformer system is shown in Fig. 8.

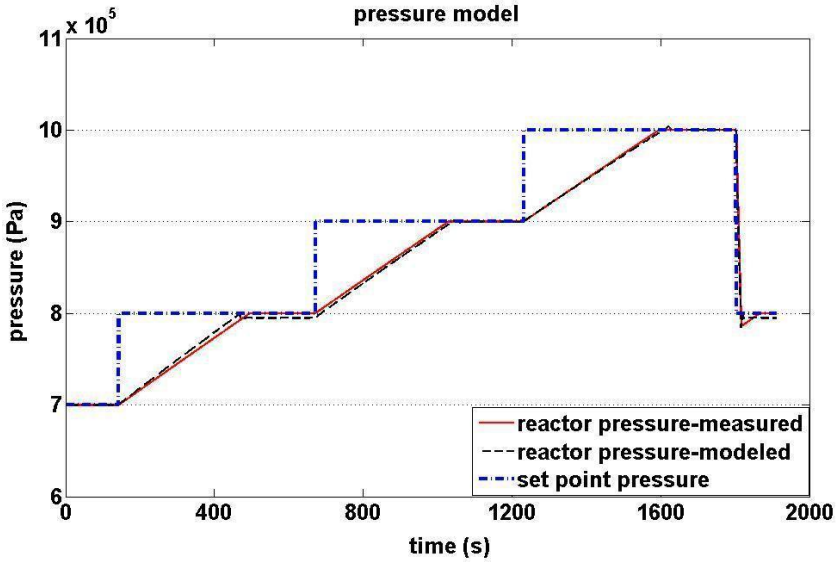

Fig. 8. Measured and simulated reactor pressures in the pressure change dynamic tests. T=923 K, F_F=200 µl/min.

It is clear that the results of simulation of reactor pressure by means of the ideal gas law fit the measurement very well.

As mentioned before, the hydrogen partial pressure difference at the retentate and permeate sides is the driving force for hydrogen permeation, which is stated by the Sieverts' law (eq. 8). Therefore, consideration of the Sieverts' law as the base of simulation of hydrogen permeation dynamic performance is essential. The simulated dynamic performance of the reforming system in the case of pressure change dynamic tests is shown in Fig. 9.

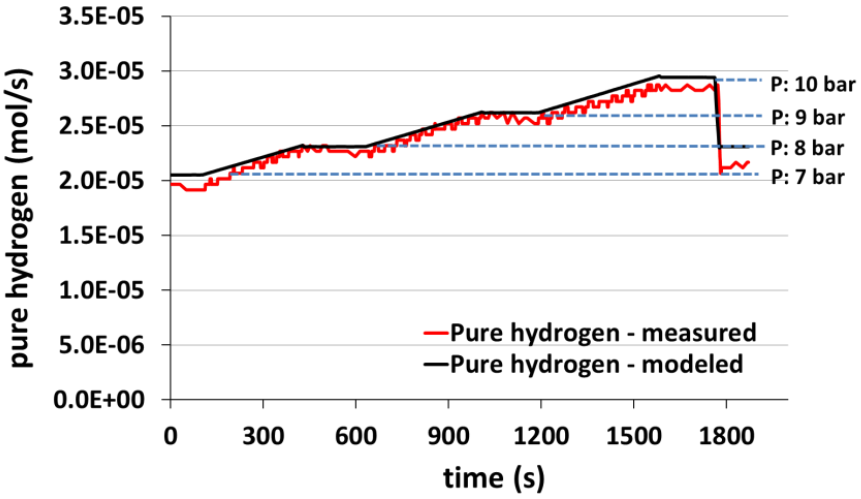

Fig. 9. Simulation of the dynamics of the pure hydrogen production rate for pressure change tests. T=923 K, F_F=200 µl/min.

The small fluctuations of the pure hydrogen measurement during the experiments are attributed to the small variations of the pressure inside the reactor, as the pressure valve acts on the outlet retentate stream. This fluctuation is ca. 10^{-6} mol/s of pure hydrogen. As expected, at constant temperature and fuel flow rate, pure hydrogen production rate follows the variation of reactor pressure by time. The CMR time constant in the case of pressure change tests was 200 seconds. The simulation of the pressure change steps fitted the experimental observation very well, proving the successful modeling and application of the Sieverts' law.

3.2.2. Fuel flow rate change simulation

In comparison with the pressure change models, it is more essential to develop a model on the fuel flow rate change. The importance of fuel flow rate change model lies in the fact that acting on fuel flow rate is much faster than the operating pressure. The CMR time constant (eq. 14) in

554 the fuel flow rate change tests was 55 seconds, which is nearly four times shorter than the
555 pressure change tests (200 seconds). The simulation result of the pure hydrogen production
556 rate for fuel flow rate change tests is presented in Fig. 10.
557

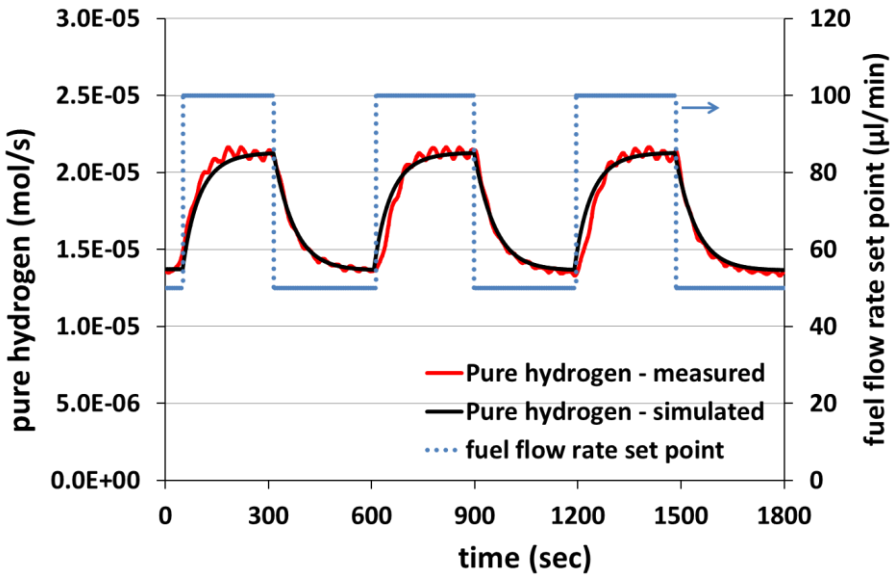

558
559
560 Fig. 10 . Simulation of the dynamics of the pure hydrogen production rate for fuel flow rate
561 change tests. T=923 K, P=10 bar.

562
563 The Sieverts' law simulation results in the case of the fuel flow rate change (Fig. 10) fitted very
564 well to the experimental observation. This is an outstanding result since the accuracy of the
565 prediction of the pure hydrogen dynamics together with fast response of the reforming system to
566 the fuel flow rate adjustments can build up a robust essential step toward further control studies.
567
568 The isothermal dynamic simulation of pure hydrogen production via ESR in the CMR
569 considering the fuel flow rate and pressure changes can play an essential role for a general
570 model of the dynamic performance of the system when connecting to a fuel cell for its online
571 feeding and control. The simulations presented in this work were able to predict the dynamics of

hydrogen permeation rate with high accuracy; however, the significance of the simulation based on fuel flow rate modifications lies in the faster response of the reformer to reach the steady state regarding the new set point.

4. Conclusion

Ethanol steam reforming (ESR) over Pd-Rh/CeO_2 catalyst was performed in a CMR at 923 K, 6-10 bar, and fuel flow rates of 50 to 200 µl/min using a mixture of ethanol and distilled water. A static model was proposed based on the Arrhenius law to calculate the molar production rate of ESR products inside the reactor (catalytic zone). The pure hydrogen production rate at steady state conditions was simulated by means of Sieverts' law model. Finally, the dynamics of the pure hydrogen production rate (permeation zone) in the case of the operating fuel flow rate or pressure set point adjustment was simulated under the ideal gas law assumptions at isothermal conditions. The effective critical factors such as hydrogen partial pressure in the CMR and the influence of the co-existence of the ESR products on the permeation behavior of the membrane were taken into account by the Sieverts' law model. Both pressure and fuel flow rate change steps simulations fitted the experimental values very well. However, the simulation of the dynamics of the fuel flow rate change was more essential, as the system responds much faster to such an adjustment. The future work will be devoted to the simulation of the startup and shut down dynamics, the effect of the composition of the inlet fuel, and the temperature profile aiming to provide a controlling system.

Acknowledgements

Funding from MINECO project ENE2015-63969-R is acknowledged. A.H. gratefully acknowledges Erasmus Mundus Joint Doctoral Program SELECT+. J.L. is Serra Húnter Fellow and is grateful to ICREA Academia program.

References

[1] Jian Q, Zhao Y, Wang H. An experimental study of the dynamic behavior of a 2 kW proton exchange membrane fuel cell stack under various loading conditions. Energy 2015;80:740–5.

[2] Carton JG, Lawlor V, Olabi AG, Hochenauer C, Zauner G. Water droplet accumulation and motion in PEM (Proton Exchange Membrane) fuel cell mini-channels. Energy 2012;39:63–73.

[3] Sharaf OZ, Orhan MF. An overview of fuel cell technology: Fundamentals and applications. Renewable and Sustainable Energy Reviews 2014;32:810–53.

[4] BOETTNER D. Proton exchange membrane (PEM) fuel cell-powered vehicle performance using direct-hydrogen fueling and on-board methanol reforming. Energy 2004;29:2317–30.

[5] Huang Z-M, Su A, Liu Y-C. Hydrogen generator system using Ru catalyst for PEMFC (proton exchange membrane fuel cell) applications. Energy 2013;51:230–6.

[6] Commission E. Comunication from the commission to the European parliament, the council, the European economic and social committee and the committee of the region. 2011.

[7] Llorca J. Microreactors for the generation of hydrogen from ethanol. In: WH L, VG C, editors. Handbook of sustainable energy, New York, USA: NOVA Publication; 2010, p. 693–9.

[8] Deluga GA, Salge JR, Schmidt LD, Verykios XE. Renewable hydrogen from ethanol by autothermal reforming. Science (New York, NY) 2004;303:993–7.

[9] Philpott BJE. Hydrogen Diffusion Technology, commercial applications of palladium membranes. Platinum Metals Review 1985:12–6.

[10] Koch R, López E, Divins NJ, Allué M, Jossen A, Riera J, et al. Ethanol catalytic membrane reformer for direct PEM FC feeding. International Journal of Hydrogen Energy 2013;38:5605–15.

[11] Hou K, Hughes R. The effect of external mass transfer, competitive adsorption and coking on hydrogen permeation through thin Pd/Ag membranes. Journal of Membrane Science 2002;206:119–30.

[12] Unemoto A, Kaimai A, Sato K, Otake T, Yashiro K, Mizusaki J, et al. The effect of co-existing gases from the process of steam reforming reaction on hydrogen permeability of palladium alloy membrane at high temperatures. International Journal of Hydrogen Energy 2007;32:2881–7.

[13] Patrascu M, Sheintuch M. On-site pure hydrogen production by methane steam reforming in high flux membrane reactor: Experimental validation, model predictions and membrane inhibition. Chemical Engineering Journal 2015;262:862–74.

[14] Gallucci F, Chiaravalloti F, Tosti S, Drioli E, Basile A. The effect of mixture gas on hydrogen permeation through a palladium membrane: Experimental study and theoretical approach. International Journal of Hydrogen Energy 2007;32:1837–45.

[15] Li A, Liang W, Hughes R. The effect of carbon monoxide and steam on the hydrogen permeability of a Pd/stainless steel membrane. Journal of Membrane Science 2000;165:135–41.

[16] Peters T a., Stange M, Klette H, Bredesen R. High pressure performance of thin Pd-

23%Ag/stainless steel composite membranes in water gas shift gas mixtures; influence of dilution, mass transfer and surface effects on the hydrogen flux. Journal of Membrane Science 2008;316:119–27.

[17] Amandusson H, Ekedahl L-G, Dannetun H. The effect of CO and O2 on hydrogen permeation through a palladium membrane. Applied Surface Science 2000;153:259–67.

[18] Mejdell AL, Chen D, Peters TA, Bredesen R, Venvik HJ. The effect of heat treatment in air on CO inhibition of a ~3μm Pd–Ag (23wt.%) membrane. Journal of Membrane Science 2010;350:371–7.

[19] Catalano J, Giacinti Baschetti M, Sarti GC. Influence of the gas phase resistance on hydrogen flux through thin palladium–silver membranes. Journal of Membrane Science 2009;339:57–67.

[20] Barreiro MM, Maroño M, Sánchez JM. Hydrogen permeation through a Pd-based membrane and RWGS conversion in H2/CO2, H2/N2/CO2 and H2/H2O/CO2 mixtures. International Journal of Hydrogen Energy 2014;39:4710–6.

[21] Cornaglia L, Múnera J, Lombardo E. Recent advances in catalysts, palladium alloys and high temperature WGS membrane reactors. International Journal of Hydrogen Energy 2015;40:3423–37.

[22] Zhang C, Liu Z, Zhou W, Chan SH, Wang Y. Dynamic performance of a high-temperature PEM fuel cell – An experimental study. Energy 2015;90:1949–55.

[23] García VM, López E, Serra M, Llorca J. Dynamic modeling of a three-stage low-temperature ethanol reformer for fuel cell application. Journal of Power Sources 2009;192:208–15.

[24] García VM, López E, Serra M, Llorca J, Riera J. Dynamic modeling and controllability analysis of an ethanol reformer for fuel cell application. International Journal of Hydrogen Energy 2010;35:9768–75.

[25] Funke M, Kühl H-D, Faulhaber S, Pawlik J. A dynamic model of the fuel processor for a residential PEM fuel cell energy system. Chemical Engineering Science 2009;64:1860–7.

[26] Jahn H-J, Schroer W. Dynamic simulation model of a steam reformer for a residential fuel cell power plant. Journal of Power Sources 2005;150:101–9.

[27] Stamps AT, Gatzke EP. Dynamic modeling of a methanol reformer—PEMFC stack system for analysis and design. Journal of Power Sources 2006;161:356–70.

[28] Kvamsdal HM, Svendsen HF, Olsvik O, Hertzberg T. Dynamic simulation and optimization of a catalytic steam reformer. Chemical Engineering Science 1999;54:2697–706.

[29] LIN S, CHEN Y, YU C, LIU Y, LEE C. Dynamic modeling and control structure design of an experimental fuel processor. International Journal of Hydrogen Energy 2006;31:413–26.

[30] Tsourapas V, Sun J, Nickens A. Modeling and dynamics of an autothermal JP5 fuel reformer for marine fuel cell applications. Energy 2008;33:300–10.

[31] López E, Divins NJ, Llorca J. Hydrogen production from ethanol over Pd–Rh/CeO2 with a metallic membrane reactor. Catalysis Today 2012;193:145–50.

[32] Idriss H, Scott M, Llorca J, Chan SC, Chiu W, Sheng P-Y, et al. A phenomenological study of the metal-oxide interface: the role of catalysis in hydrogen production from renewable resources. ChemSusChem 2008;1:905–10.

[33] Domínguez M, Taboada E, Molins E, Llorca J. Ethanol steam reforming at very low temperature over cobalt talc in a membrane reactor. Catalysis Today 2012;193:101–6.

[34] Hedayati A, Le Corre O, Lacarrière B, Llorca J. Exergetic study of catalytic steam reforming of bio-ethanol over Pd–Rh/CeO2 with hydrogen purification in a membrane reactor. International Journal of Hydrogen Energy 2015;40:3574–81.

[35] Reb Research & Consulting, accessed on 2015-09-23, http://www.rebresearch.com/ 2015.

[36] Divins NJ, López E, Rodríguez Á, Vega D, Llorca J. Bio-ethanol steam reforming and autothermal reforming in 3-μm channels coated with RhPd/CeO2 for hydrogen generation. Chemical Engineering and Processing: Process Intensification 2013;64:31–7.

[37] Hedayati A, Le Corre O, Lacarrière B, Llorca J. Experimental and exergy evaluation of ethanol catalytic steam reforming in a membrane reactor. Catalysis Today 2016;IN PRESS.

[38] López E, Divins NJ, Anzola A, Schbib S, Borio D, Llorca J. Ethanol steam reforming for hydrogen generation over structured catalysts. International Journal of Hydrogen Energy 2013;38:4418–28.

[39] Basile A. Hydrogen Production Using Pd-based Membrane Reactors for Fuel Cells. Topics in Catalysis 2008;51:107–22.

[40] Hla SS, Morpeth LD, Dolan MD. Modelling and experimental studies of a water-gas shift catalytic membrane reactor. Chemical Engineering Journal 2015;276:289–302.

[41] Basile A, Curcio S, Bagnato G, Liguori S, Jokar SM, Iulianelli A. Water gas shift reaction in membrane reactors: Theoretical investigation by artificial neural networks model and experimental validation. International Journal of Hydrogen Energy 2015;40:5897–906.

[42] Sanz R, Calles JA, Alique D, Furones L, Ordóñez S, Marín P. Hydrogen production in a Pore-Plated Pd-membrane reactor: Experimental analysis and model validation for the Water Gas Shift reaction. International Journal of Hydrogen Energy 2015;40:3472–84.

[43] Di Marcoberardino G, Sosio F, Manzolini G, Campanari S. Fixed bed membrane reactor for hydrogen production from steam methane reforming: Experimental and modeling approach. International Journal of Hydrogen Energy 2015;40:7559–67.

[44] Iulianelli A, Liguori S, Huang Y, Basile A. Model biogas steam reforming in a thin Pd-supported membrane reactor to generate clean hydrogen for fuel cells. Journal of Power Sources 2015;273:25–32.

[45] Chein RY, Chen YC, Chyou YP, Chung JN. Three-dimensional numerical modeling on high pressure membrane reactors for high temperature water-gas shift reaction. International Journal of Hydrogen Energy 2014;39:15517–29.

[46] Papadias DD, Lee SHD, Ferrandon M, Ahmed S. An analytical and experimental investigation of high-pressure catalytic steam reforming of ethanol in a hydrogen selective membrane reactor. International Journal of Hydrogen Energy 2010;35:2004–17.

[47] Jakobsen, A. H. Chemical Reactor Modeling: Multiphase Reactive Flows. 2nd ed. London: Springer; 2014.